



Design and Synthesis of AIE-Based Small-Molecule and Nanofibrous Film for Fluorescent Sensing Application

Chunping Ma^{1,2}, Zhiyi Li¹, Chenglin Zhang³, Gaoyi Xie^{3*}, Yancheng Wu¹, Yangfan Zhang¹, Jinpeng Mo¹, Xi Liu^{1*}, Ke Wang⁴, Dong Xie⁴ and Yang Li^{2*}

¹Guangdong-Hong Kong Joint Laboratory for New Textile Materials, School of Textile Materials and Engineering, Wuyi University, Jiangmen, China, ²School of Materials and Energy Engineering, Guizhou Institute of Technology, Guiyang, China, ³School of Biotechnology and Health Sciences, Wuyi University, Jiangmen, China, ⁴Institute of Bioengineering, Guangdong Academy of Sciences, Guangzhou, China

OPEN ACCESS

Edited by:

Haichang Zhang,
Qingdao University of Science and
Technology, China

Reviewed by:

Cheng Zhou,
National University of Singapore,
Singapore
Zhu Mao,
Shenzhen Institutes of Advanced
Technology (CAS), China

*Correspondence:

Gaoyi Xie
xiegaoyi@126.com
Xi Liu
liuxi_wyu@163.com
Yang Li
20130214@git.edu.cn

Specialty section:

This article was submitted to
Organic Chemistry,
a section of the journal
Frontiers in Chemistry

Received: 19 June 2021

Accepted: 06 July 2021

Published: 06 August 2021

Citation:

Ma C, Li Z, Zhang C, Xie G, Wu Y, Zhang Y, Mo J, Liu X, Wang K, Xie D and Li Y (2021) Design and Synthesis of AIE-Based Small-Molecule and Nanofibrous Film for Fluorescent Sensing Application. *Front. Chem.* 9:727631. doi: 10.3389/fchem.2021.727631

Fluorescent sensors that respond to environmental conditions (temperature, pressure, and pH) have attracted widespread attention in recent years. Generally, traditional solid-state fluorescent materials tend to suffer from aggregation-induced quenching (ACQ) and difficulty of film forming, limiting their extensive applications. Therefore, researchers are focusing more and more attention on fluorescent sensors with aggregation-induced emission (AIE) effects. Herein, the article reports an AIE molecule (TPEBZMZ) containing tetraphenylethylene (TPE) and benzimidazole fragments. The fluorescence properties of TPEBZMZ in solution and aggregation states have been investigated, and the luminescence performance and aggregation structures of solid-state TPEBZMZ after force and acid treatments have been explored. The results show obvious AIE and fluorescent sensing properties of TPEBZMZ, presenting force- and acid-induced discolorations. Moreover, the TPEBZMZ-based fluorescent nanofibrous film is fabricated by electrospinning the solution of TPEBZMZ blended with polylactic acid (PLA), which shows a good nanofiber film structure and exhibits reversible acid-induced discoloration property, even with only 0.5 wt% TPEBZMZ. This work provides a simple strategy to achieve stimulus-responsive fluorescent film.

Keywords: fluorescent sensing, AIE, nanofibrous film, acid-induced discoloration, luminescence performance

INTRODUCTION

Fluorescent films composed of π -conjugated materials-based fluorescent sensors and membranous materials are promising sensor technology due to their real-time detection, easy fabrication, non-invasiveness detection, and mechanical stability and flexibility (Guan et al., 2015; Miao et al., 2016). In recent years, they have been widely used in detecting residual pesticides (Peng et al., 2021), enzymes (Zhao et al., 2017a; Zhao et al., 2017b), pollutants (Lee et al., 2019; Zhao et al., 2020b; Sun et al., 2021), explosives (Zhou et al., 2014; Sun et al., 2015; Li et al., 2018; Hao et al., 2021), metal ions (Chen et al., 2020), gases (Moscoso et al., 2020), and temperature and humidity (Jiang et al., 2020; Li et al., 2020), which greatly expanded the applications of fluorescence sensors. Generally, high selectivity and sensitivity are the key characteristics of a successful membranous fluorescent sensor (Sun et al., 2015). Selectivity is mainly related to the specific interaction between fluorescent probe and environmental stimulus or detection objects (Zhou et al., 2017), showing differentiated luminescence characteristics, while sensitivity is primarily determined by fluorescence intensity

(Song et al., 2015). Traditional fluorescent materials usually present weak fluorescence in the solid state but high fluorescence in solution due to the widely known aggregation-caused quenching (ACQ) effect. ACQ greatly limits the application of traditional fluorescence materials (Hong et al., 2011). Aggregation-induced emission (AIE), proposed by Tang's research team in 2001, can be used as a perfect solution to the ACQ issue (Luo et al., 2001). AIE behavior is just the opposite of the ACQ fluorescence behavior of traditional fluorescent compounds: AIE luminogen (AIEGen) emits weak fluorescence in solution, whereas it emits strong fluorescence when aggregated or in a solid state (Luo et al., 2001). The AIE phenomenon is related to intermolecular rotation, restricting these rotations in solid state, inducing the fluorescent emission of the corresponding compound (Qin et al., 2012; Liu et al., 2019; Zhao et al., 2020a). Therefore, AIEGen-based films will show specifically emissive characteristics. Thus, AIEGen-based fluorescent films will provide an effective strategy for the development of fluorescent film sensors.

Electrospinning is an effective method to obtain polymer-based nanofibrous films, compared with casting films, showing a larger specific surface area and higher porosity (Xue et al., 2019). Thus, fluorescent films fabricated by electrospinning can improve the sensitivity and response rate (Zhao et al., 2017b). Therefore, much attention has been devoted to nanofibrous fluorescent films to explore their specific sensing properties. For example, Li et al. (2019) have developed an epoxy resin system functionalized with the typical AIE tetraphenylethylene (TPE) groups, forming nanofibrous films by electrospinning, and finally obtained temperature-sensitive fluorescent films probes. Yang et al. (Yang et al., 2018) have reported specific composite nanofibrous films by electrospinning of AIE small molecules (oME-TPA) and polyvinyl alcohol (PVA) and further studied its piezochromic properties related to sensitivities. Zhao et al. (2017a) have grafted TPE derivatives and phloxine B onto electrospun nanofiber film, inducing the static quenching of phloxine B through protamine adsorption and combining them with the aggregation of TPE-based groups, promoting fluorescence emission of nanofiber, which realized effective monitoring of different concentrations of heparin. Therefore, the design and development of novel AIE molecules containing nanofiber fluorescent films will benefit the realization of efficient fluorescent sensing applications.

Herein, we report a novel compound (TPEBZMZ) containing the classic AIE group tetraphenylethylene (TPE) and benzimidazole unit. The TPE group renders the TPEBZMZ molecule AIE property, and the structure of the benzimidazole unit will offer the potential of acid-induced discoloration. The relationship between the structure, aggregate, and luminescence properties of TPEBZMZ in different states and force and acid treatments has been systematically studied. Specifically, TPEBZMZ shows an obvious AIE phenomenon and fluorescent sensing properties of force- and acid-induced discolorations. More importantly, we prepared TPEBZMZ-based fluorescent nanofibrous film by electrospinning the solution of TPEBZMZ blended with polylactic acid (PLA), and the nanofibrous film displays a good reversible acid-induced

discoloration property. Significantly, this work provides a simple strategy to prepare fluorescent sensing film.

MATERIALS AND METHODS

Materials

1-Bromo-1,2,2-triphenylethene (P₃Br) was purchased from Macklin Biochemical Co., Ltd. (Shanghai, China). 4-Formylphenylboronic acid, tetrabutylammonium bromide (TBAB), tetrakis(triphenylphosphine) palladium [Pd(PPh₃)₄], 2-(cyanomethyl) benzimidazole, and tetrabutylammonium hydroxide (TBAH) were purchased from Energy Chemical. Polylactic acid (PLA, 4032D) was purchased from NatureWorks (America). All of the above reagents were used as received. Potassium carbonate (K₂CO₃), potassium hydroxide (KOH), tetrahydrofuran (THF), ethanol, and dichloromethane (DCM) were purchased the analytical grade from Guangzhou Chemical Reagent Factory (Guangzhou, China) and used without further purification.

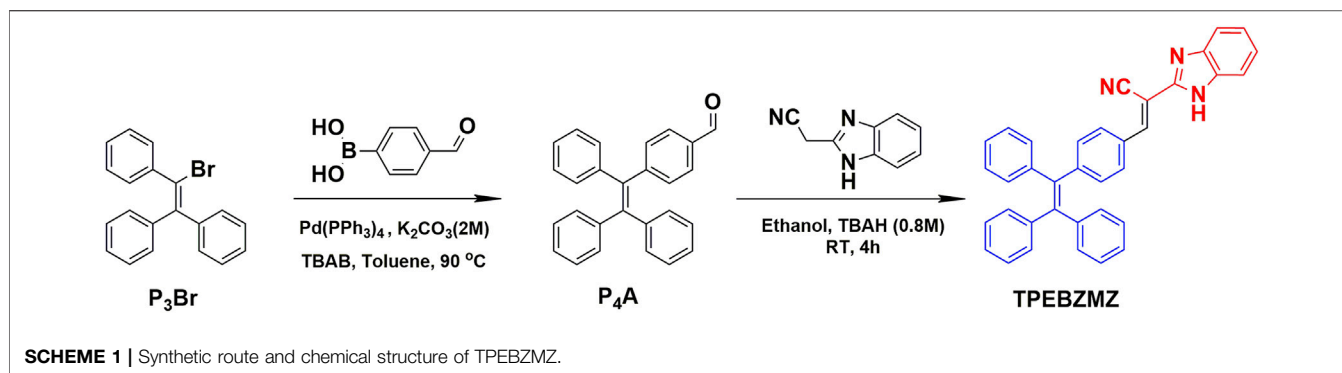
Synthesis of P₄A and (E)-2-(1H-Benzo[d]imidazol-2-yl)-3-(4-(1,2,2-triphenylvinyl)phenyl) Acrylonitrile (TPEBZMZ)

The intermediate of P₄A was synthesized according to a previous literature method (Xu et al., 2013).

P₄A (1.080 g, 3 mmol), 2-(cyanomethyl) benzimidazole (0.471 g, 3 mmol), and ethanol (20 ml) were mixed and stirred in a 50 ml two-necked round-bottomed flask at room temperature. After adding tetrabutylammonium hydroxide (TBAH, 0.8 M, 10 drops) dropwise, the mixture was stirred continually at room temperature for 4 h. The precipitate was filtrated and washed three times using ethanol, resulting in a yellow powder (1.087 g, yield 72.6%). ¹H NMR (500 MHz, CDCl₃) δ (ppm): 9.58 (s, 1 H), 8.41 (s, 1 H), 7.77 (d, 2 H, J = 8.32 Hz), 7.34 (dd, 2 H, J = 3.12, 6.09 Hz), 6.01–7.23 (m, 19 H). ¹³C NMR (125 MHz, CDCl₃) δ (ppm): 148.35, 146.46, 146.34, 143.19, 143.09, 143.01, 139.81, 132.19, 131.37, 131.33, 131.29, 130.55, 129.61, 127.99, 127.95, 127.71, 127.12, 126.86, 117.01, 98.63. FT-IR (KBr): 2924, 2854, 1593, 1491, 1443, 747, 700, 616. ESI-MS, m/z: 500.21 ([M + H]⁺, calcd for C₃₆H₂₆N₃, 500.20).

Characterization

¹H NMR and ¹³C NMR spectra were recorded on a Bruker AVANCE NEO 500 spectrometer. Mass spectra were measured on an LTQ Orbitrap LCMS spectrometer. FT-IR spectra were recorded using Nicolet iS5 spectrometer (KBr pellet). UV-visible absorption spectra (UV-vis) were obtained via a SHIMADZU UV-2700 spectrophotometer. Fluorescence spectra (PL) were determined by a Shimadzu RF-6000 spectrometer with a slit width of 3 nm for excitation and 5 nm for emission. Thermal behaviors were studied using differential scanning calorimetry (DSC) on a NETZSCH thermal analyzer (DSC214Polyma) with both heating and cooling rates of 20°C/min under a N₂ atmosphere. Powder X-ray diffraction (PXRD) measurements were carried out at 298 K on a Rigaku X-ray



diffractometer (Ultima IV, Japan) with an X-ray source of Cu K α ($\lambda = 0.1541$ nm) at 40 kV and 40 mA, at a scan rate of $5^\circ(2\theta)/\text{min}$ from 5° to 60° . The frontier molecular orbital distributions of TPEBZMZ and acid fumed TPEBZMZ (TPEBZMZ-HCl) were determined using density functional theory (DFT) using Gaussian 09 at the B3LYP/6-311G(d,p) level. After 1 min of gold coating, the surface morphologies of nanofibers were observed by a scanning electron microscope (Sigma 500, Zeiss, German) equipped with an in-lens detector at 15 kV. Fluorescent microscopic images were recorded on a laser confocal microscope (Leica DMI8, German) in an XY scan mode, using an argon ion laser source with a wavelength of 488 nm.

Electrospinning Process of PLA-TPEBZMZ and PLA Nanofibrous Films

The electrospinning process was performed on an E05 electrospinning apparatus (supplied by Lepton Technology Co., Ltd., Foshan, China), using a 10 wt% PLA/(DMF:DCM = 1:2) solution with or without 0.05 wt% TPEBZMZ as a spinning solution. The nanofibers were collected by a rotating metal cylinder (100 r/min) covered with release paper, with an immobile distance of 20 cm away from the needle tip of the spinneret (0.7 mm inner diameter). The spinning voltage and fluid flow rate were set to 12 kV and 2 ml/h, respectively. The obtained nanofibrous films were dried in a vacuum oven at 70°C for another 12 h to remove the residual solvent completely.

RESULT AND DISCUSSION

Synthesis and Characterization

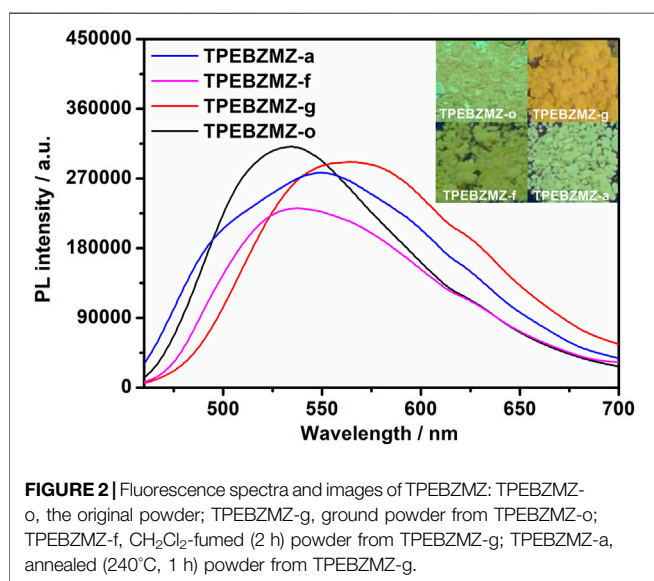
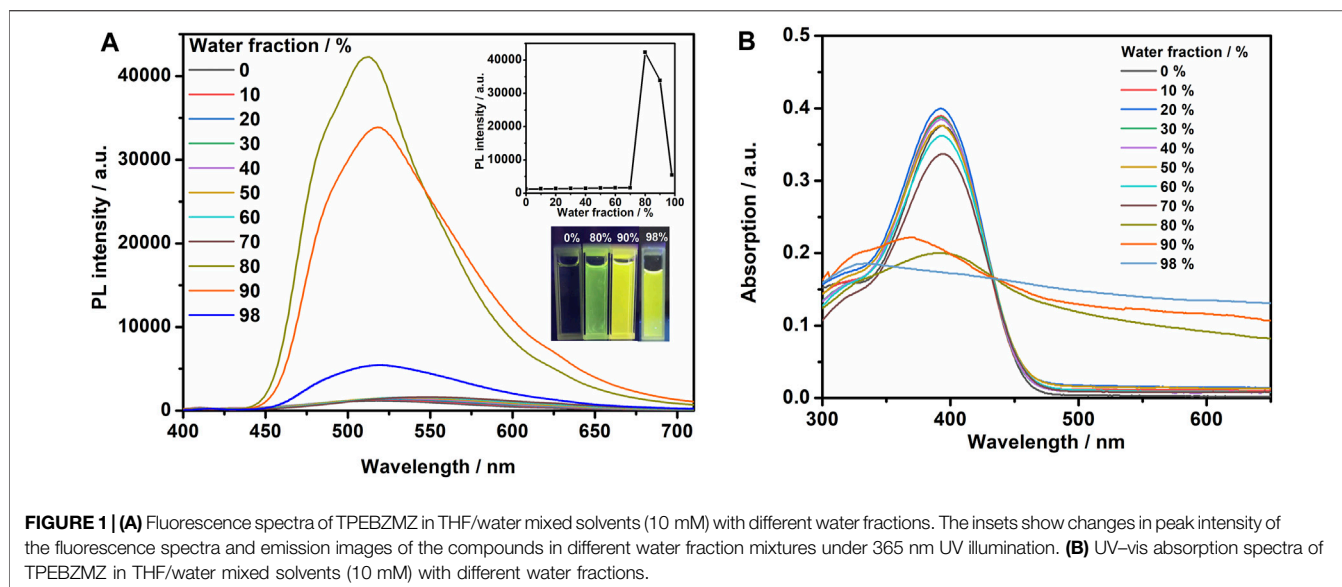
The synthetic route of TPEBZMZ is shown in **Scheme 1**. The intermediate molecule P_4A was acquired *via* Suzuki coupling from P_3Br and 4-formylphenylboronic acid. The final product TPEBZMZ was obtained by Knoevenagel reaction with P_4A and 2-(cyanomethyl) benzimidazole. As shown in **Supplementary Figures 1–4**, TPEBZMZ was characterized using ^1H NMR and ^{13}C NMR spectroscopies, mass spectrometry, and Fourier transform infrared spectroscopy, confirming that the target compound TPEBZMZ has been successfully synthesized. The thermal stability of TPEBZMZ was investigated by thermal

gravity analysis (TGA) under a nitrogen atmosphere, and the result is presented in **Supplementary Figure 5**. TPEBZMZ showed good thermal stability with 5% weight loss at a temperature (T_d) of 366°C .

AIE Property of TPEBZMZ

Due to the state-of-the-art AIE functional unit, TPE, we proposed that the TPEBZMZ molecule can exhibit the AIE effect, which was firstly examined by the photoluminescence (PL) fluorescence emission spectra of TPEBZMZ/THF/ H_2O solutions with different water content. The resulting spectra, the plot of PL intensity vs. water fraction, and the fluorescence photo images of specific water fraction are shown in **Figure 1A**. The fluorescence emission of the TPEBZMZ/THF solution in the presence of only the good solvent THF is very weak, and the fluorescence of the solution is almost invisible to the naked eye. When the water content is lower than 70%, the fluorescence spectra show few changes. In contrast, the fluorescence intensity increases sharply, when the water content reaches 80%, and the fluorescence intensity is about 36 times compared to 0% water content. The fluorescence intensity begins to decrease after the water content is further increased to 90%, within a sharp drop of fluorescence intensity at 98% of water content. We speculate that the reason for the change in fluorescence intensity is because TPEBZMZ aggregation started with 80% of water content, and the size of aggregates increased gradually when the water fraction increased to 98%, leading to a remarkable light scattering phenomenon (Thomas et al., 2007). Thus, the PL fluorescence experiment preliminarily confirmed the AIE property of TPEBZMZ.

Optical absorption properties of TPEBZMZ/THF/ H_2O solutions with different water content were investigated using UV–vis absorption spectroscopy. As shown in **Figure 1B**, the solution absorption spectra exhibit similar characteristics under 0–70% water content, while the obvious decreases of absorption intensities were demonstrated in >80% water content solutions. Moreover, the spectra of >80% water content show the obvious tailing phenomenon in absorption curves, especially presented in the 98% water content solution, which can be attributed to the Mie scattering effect of nano aggregates (Zhang et al., 2015). The tendency of absorption spectra is consistent with the results of fluorescence emission spectra of TPEBZMZ/THF/ H_2O mixture solution with different water content. These results further



confirmed that TPEBZMZ shows the AIE effect, which will benefit its further fluorescent sensor application.

Mechanochromism Property of TPEBZMZ

To evaluate the stimulus-response characteristic of TPEBZMZ, we first tested the fluorescence performance of the original TPEBZMZ (TPEBZMZ-o) powder. As shown in **Figure 2**, TPEBZMZ-o shows a strong yellow-green fluorescence emission with a PL peak at 534 nm. The ground powder (TPEBZMZ-g) was obtained by grinding TPEBZMZ-o, which releases an orange-yellow fluorescence emission with a PL peak of 565 nm. The 31 nm red shift of fluorescence peaks of TPEBZMZ-o and TPEBZMZ-g demonstrated that the preliminary mechanochromism property of TPEBZMZ. The fluorescence

color returned to yellow-green when the TPEBZMZ-g sample was treated with dichloromethane (DCM) fumigation (TPEBZMZ-f), and TPEBZMZ-f shows a blue-shift fluorescence spectrum, showing a similar wavelength range of TPEBZMZ-o. The annealed sample (TPEBZMZ-a) of TPEBZMZ-g also exhibits a similar effect with a blue-shift of fluorescence spectrum. Moreover, the results of the cycling measurement (**Supplementary Figure 6**) indicate that TPEBZMZ displays good reversible mechanochromism properties.

Solid-state TPEBZMZ changes from yellow-green to orange-yellow after being mechanically stimulated. We speculate that the reason is the change in the aggregation state of the TPEBZMZ molecules due to the action of external mechanical forces (Ma et al., 2016; Ma et al., 2017). Accordingly, the aggregate structures of the TPEBZMZ powder with different treatments were investigated by powder X-ray diffraction (PXRD) measurements. As shown in **Figure 3A**, a large number of sharp diffraction peaks appeared in the PXRD curve of TPEBZMZ-o, suggesting a relatively regular molecular arrangement and good crystallinity presented in the initial state of TPEBZMZ. While the ground sample TPEBZMZ-g shows weak and even disappeared diffraction peaks, it indicates a relatively disordered and amorphous state exhibited in the TPEBZMZ-g sample. Moreover, the diffraction peaks are partially restored while TPEBZMZ-g is annealed, and the major peaks of the fumed TPEBZMZ-f are also restored and similar to those of TPEBZMZ-o. These results demonstrated the varied aggregated structures of TPEBZMZ with different treatments, which is consistent with its mechanochromism property.

Aggregate structures of TPEBZMZ with different treatments were further characterized by differential scanning calorimetry (DSC) measurements. As shown in **Figure 3B**, in the first heating curves, TPEBZMZ-o shows an obvious melting peak at 298°C (enthalpy of 25.80 J/g), while TPEBZMZ-g displays a weak melting peak at 290°C with an enthalpy of 4.63 J/g, suggesting

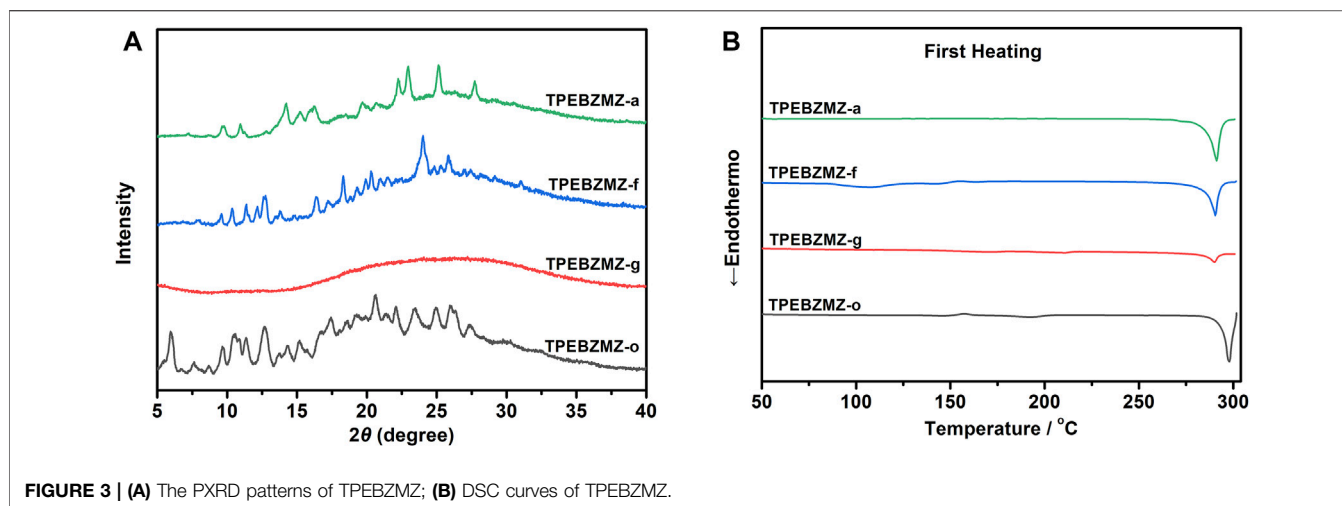


FIGURE 3 | (A) The PXRD patterns of TPEBZMZ; (B) DSC curves of TPEBZMZ.

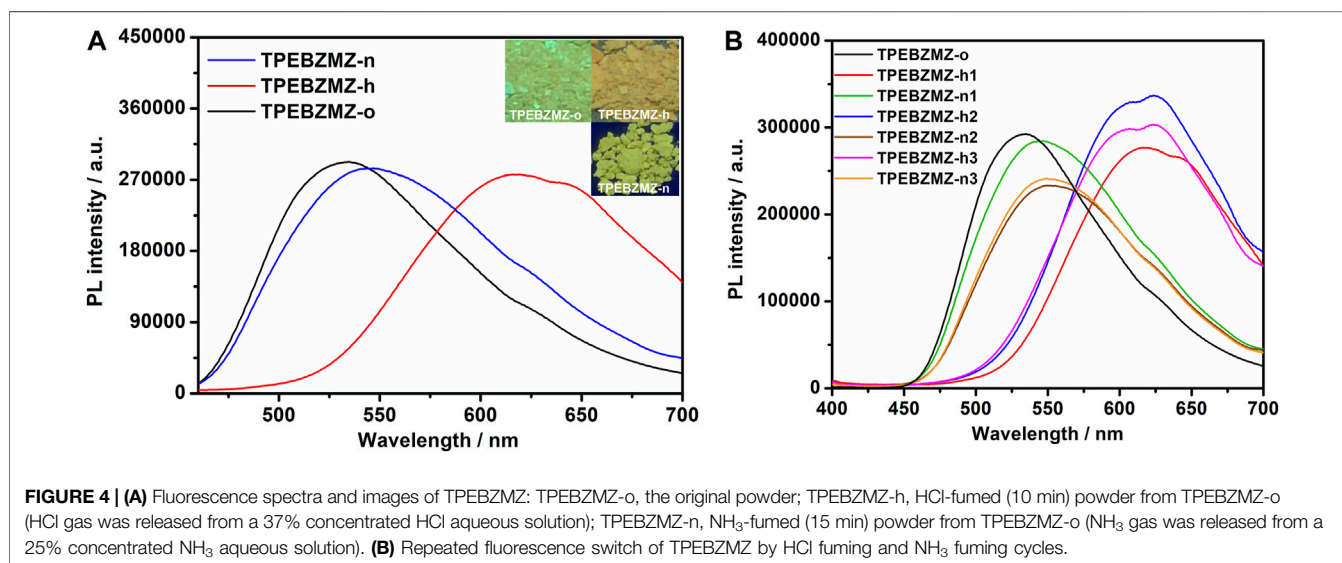


FIGURE 4 | (A) Fluorescence spectra and images of TPEBZMZ: TPEBZMZ-o, the original powder; TPEBZMZ-h, HCl-fumed (10 min) powder from TPEBZMZ-o (HCl gas was released from a 37% concentrated HCl aqueous solution); TPEBZMZ-n, NH_3 -fumed (15 min) powder from TPEBZMZ-o (NH_3 gas was released from a 25% concentrated NH_3 aqueous solution). (B) Repeated fluorescence switch of TPEBZMZ by HCl fuming and NH_3 fuming cycles.

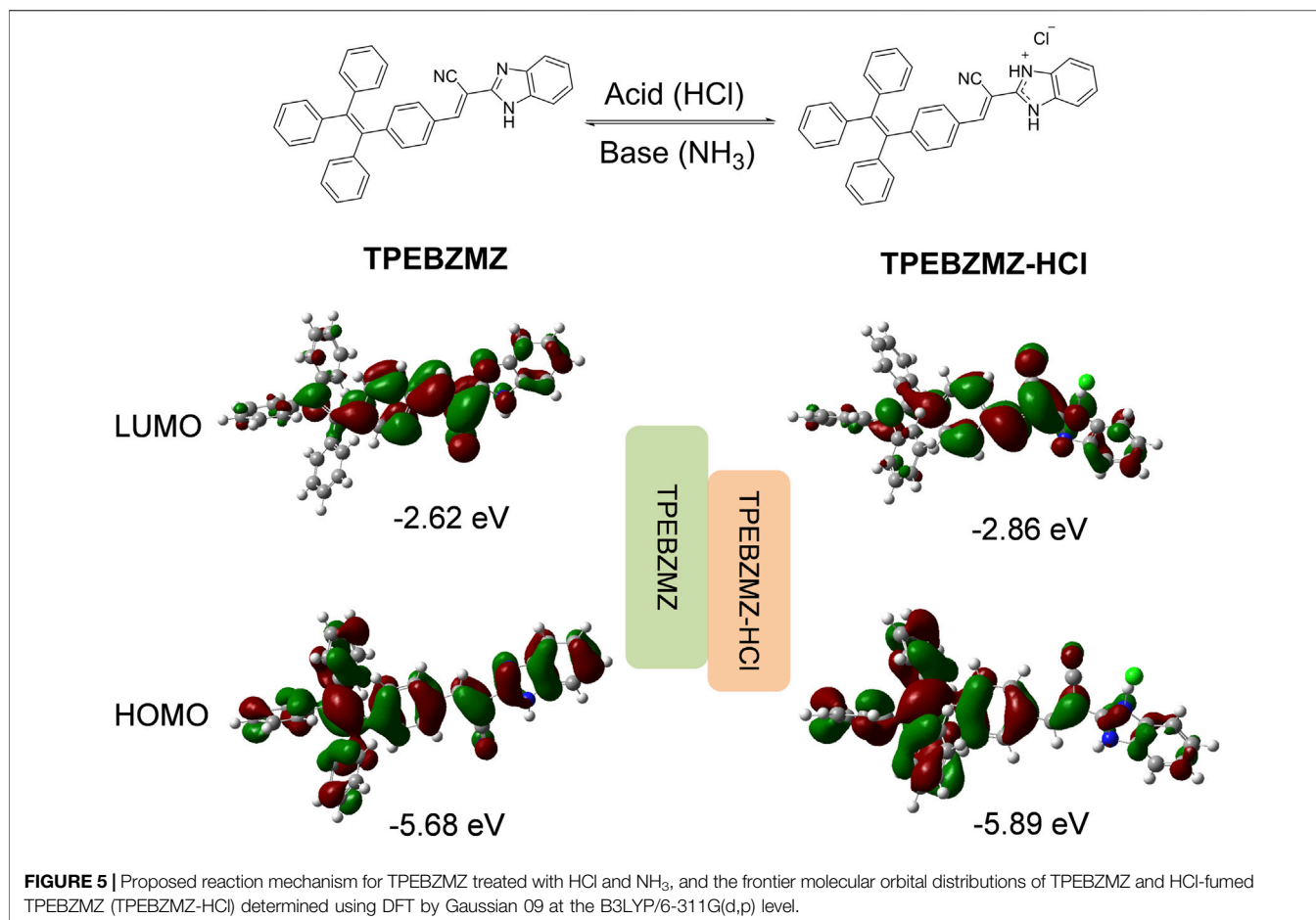
that the mainly amorphous state is presented in the TPEBZMZ-g sample. TPEBZMZ-f and TPEBZMZ-a also have obvious crystal melting peaks near 290°C , but the melting enthalpies (23.77 J/g and 25.90 J/g, respectively) are slightly lower than or almost the same as TPEBZMZ-o, indicating that a certain rearrangement of amorphous structure of the TPEBZMZ sample appeared under annealing or DCM fumigation treatments.

Acid-Base Discoloration Property of TPEBZMZ

The protonatable benzimidazole unit presented in the TPEBZMZ molecule renders the variable electron cloud density of TPEBZMZ after being protonated, further, in turn, affecting its fluorescence performance. Thus, TPEBZMZ-o was fumigated by hydrogen chloride gas to obtain the protonated acid-fumigated TPEBZMZ powder (TPEBZMZ-h). As shown in Figure 4A, the TPEBZMZ-h sample displays orange fluorescence

with an emission peak at 589 nm, which shows an obvious red shift of 55 nm compared to the TPEBZMZ-o solid. Furthermore, the TPEBZMZ-h solid fumigated NH_3 vapor (TPEBZMZ-n) shows a fluorescence color turning back to yellow-green, and its fluorescence spectrum is almost restored to that of TPEBZMZ-o. Figure 4B shows the repeated fluorescence spectra of TPEBZMZ by HCl fuming and NH_3 fuming cycles, displaying modest repeatability of acid-base discoloration under three cycles. These results prove that the TPEBZMZ powder exhibits good reversible acid-base discoloration performance.

The proposed reaction mechanism about TPEBZMZ treated with HCl and NH_3 is shown in Figure 5, and the frontier molecular orbital distributions of TPEBZMZ and HCl-protonated TPEBZMZ (TPEBZMZ-HCl) were further determined using DFT by Gaussian 09 at the B3LYP/6-311G(d,p) level. The electron density distribution of the lowest unoccupied molecular orbital (LUMO) of TPEBZMZ is localized in the central molecule and tends to be fastened to the cyano unit.



The highest occupied molecular orbital (HOMO) of TPEBZMZ shows a well-proportioned electron density distribution. Moreover, the electron density distributions of the LUMO and HOMO of TPEBZMZ-HCl exhibit a delocalization effect, which tends to localize in the benzimidazole hydrochloride unit and TPE unit, respectively. Correspondingly, TPEBZMZ and TPEBZMZ-HCl exhibit LUMO/HOMO levels of $-2.62/-5.68$ and $-2.86/-5.89$ eV, respectively, presenting the bandgaps of 3.06 and 3.03 eV. The red-shift fluorescence spectra of HCl-protonated TPEBZMZ could be attributed to the delocalization effect of its electron density distributions, which may explain the acid-base discoloration property of TPEBZMZ.

Fluorescent Sensing Property of TPEBZMZ-Based Nanofibrous Film

Generally, small-molecule fluorescent powders exhibit poor film-forming properties requiring expensive film-forming equipment (e.g., vacuum evaporator), which will limit their practical application (Hong et al., 2011). To overcome this drawback, TPEBZMZ was blended with a PLA dimethylformamide (DMF)/DCM mix solution by electrospinning to obtain the TPEBZMZ-based nanofibrous film (TPEBZMZ-m). The morphology of TPEBZMZ-m and a pure PLA nanofibrous

film was tested using scanning electron microscopy (SEM). The corresponding SEM images are shown in **Figures 6A–D**. TPEBZMZ-m shows an almost similar microstructure compared to that of the pure PLA nanofibrous film, both of which possess filaments with diameters of 500–800 nm.

To evaluate the fluorescent sensing property of TPEBZMZ-m, the acid-induced discoloration experiment was performed. The results of the acid-induced discoloration experiment are shown in **Figure 7A**. Unlike the pure PLA nanofibrous film (**Supplementary Figure 7B**), the nascent TPEBZMZ-m film emits significant green fluorescence under ultraviolet light (confirmed by laser confocal microscope, **Supplementary Figures 7C–E**), even with only 0.5 wt% TPEBZMZ. After fuming by HCl vapor, the resulting film (TPEBZMZ-m-h) exhibits an obvious yellow fluorescence color. Moreover, when the TPEBZMZ-m-h sample was fumed with a NH₃ vapor (TPEBZMZ-m-n), the fluorescence of the sample became green again. To quantitatively characterize the fluorescence emission wavelength of TPEBZMZ-m after different treatments, we used fluorescence spectroscopy to test the electrospinning nanofibrous film samples after different treatments. As shown in **Figure 7A**, the TPEBZMZ-m sample shows a fluorescence emission peak of 496 nm, while the TPEBZMZ-m-h sample exhibits a fluorescence emission peak

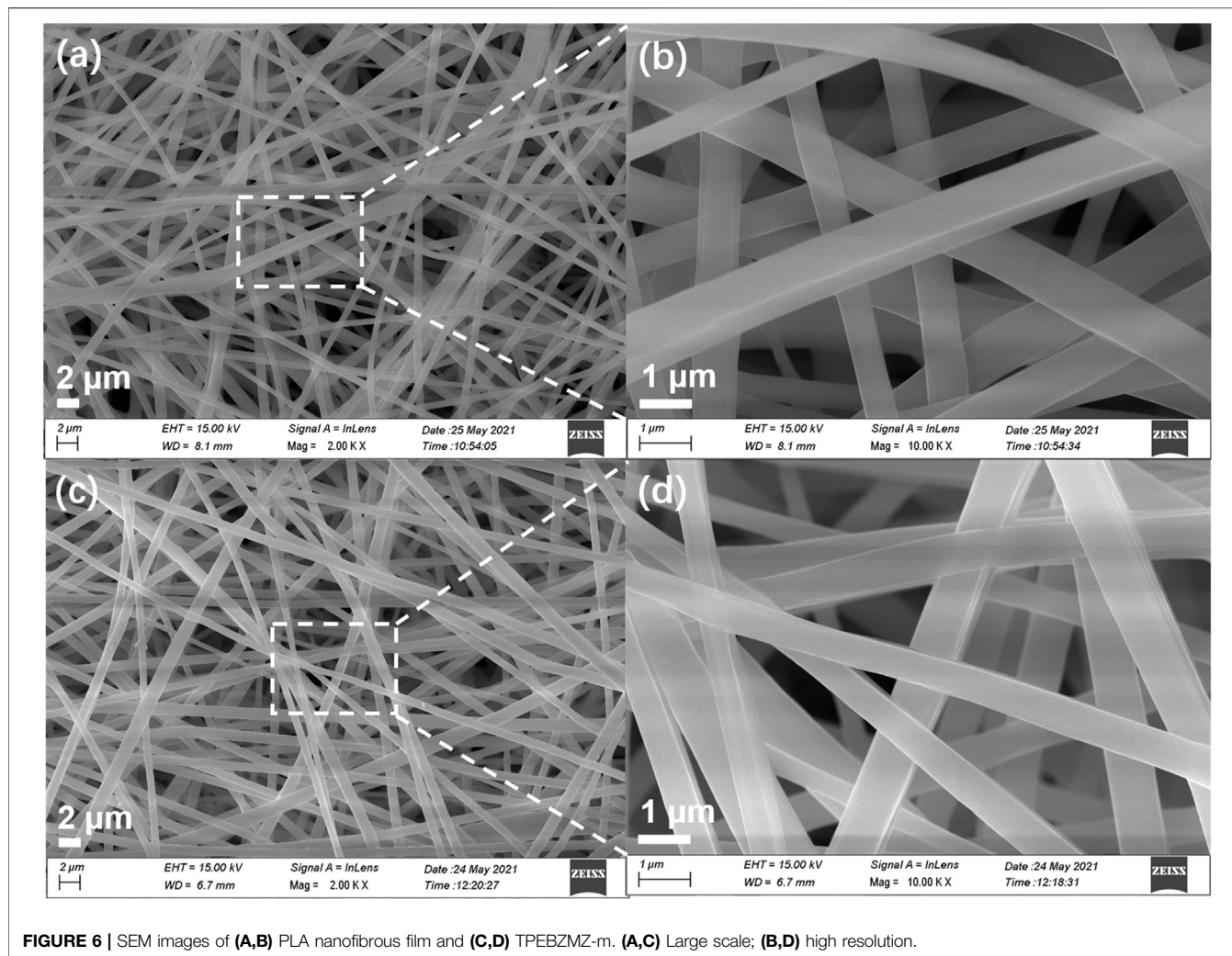


FIGURE 6 | SEM images of (A,B) PLA nanofibrous film and (C,D) TPEBZMZ-m. (A,C) Large scale; (B,D) high resolution.

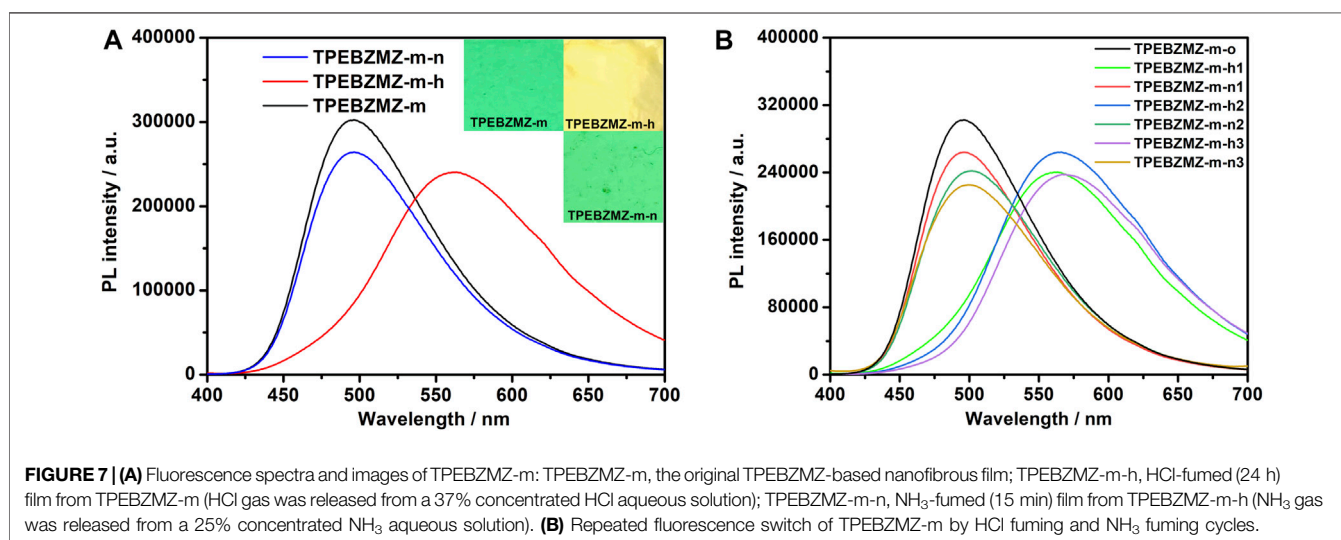


FIGURE 7 | (A) Fluorescence spectra and images of TPEBZMZ-m: TPEBZMZ-m, the original TPEBZMZ-based nanofibrous film; TPEBZMZ-m-h, HCl-fumed (24 h) film from TPEBZMZ-m (HCl gas was released from a 37% concentrated HCl aqueous solution); TPEBZMZ-m-n, NH₃-fumed (15 min) film from TPEBZMZ-m-h (NH₃ gas was released from a 25% concentrated NH₃ aqueous solution). (B) Repeated fluorescence switch of TPEBZMZ-m by HCl fuming and NH₃ fuming cycles.

of 563 nm, with a red shift of 67 nm compared to TPEBZMZ-m. Meanwhile, the TPEBZMZ-m-n sample shows an obvious blue-shift fluorescence emission compared to the TPEBZMZ-m-h sample and presenting a fluorescence emission peak at 496 nm, coinciding with the spectroscopy of TPEBZMZ-m. **Figure 7B** shows the repeated fluorescence spectra of TPEBZMZ-m by HCl fuming and NH₃ fuming cycles, displaying good repeatability of acid-base discoloration under three cycles. The well acid-base discoloration repeatability of TPEBZMZ-based nanofibrous film suggests its good potential on fluorescent film sensors application. These results demonstrated that electrospinning acts as a simple and efficient method to prepare TPEBZMZ-based nanofibrous fluorescent film with good reversible acid-induced discoloration property, which provides an effective strategy for developing fluorescent film sensors.

CONCLUSION

In conclusion, we have developed an AIE molecule (TPEBZMZ) containing tetraphenylethylene (TPE) and benzimidazole fragments, which is synthesized from 2-cyanomethylbenzimidazole and 4-(1,2,2-tristyryl) benzaldehyde. TPEBZMZ powder shows obvious AIE and fluorescent sensing properties and exhibits force- and acid-induced discoloration phenomena. More importantly, the TPEBZMZ-based fluorescent nanofibrous film is fabricated by electrospinning the solution of TPEBZMZ blended with polylactic acid (PLA), exhibiting a good nanofiber film structure and well reversible acid-induced discoloration properties. This work demonstrates a simple strategy to achieve stimulus-responsive fluorescent film, which will benefit the development of fluorescent film sensors.

REFERENCES

- Chen, M., An, J., Hu, Y., Chen, R., Lyu, Y., Hu, N., et al. (2020). Swelling-shrinking Modified Hyperstatic Hydrophilic Perovskite Polymer Fluorescent Beads for Fe(III) Detection. *Sensors Actuators B: Chem.* 325, 128809. doi:10.1016/j.snb.2020.128809
- Guan, W., Zhou, W., Lu, J., and Lu, C. (2015). Luminescent Films for Chemo- and Biosensing. *Chem. Soc. Rev.* 44, 6981–7009. doi:10.1039/c5cs00246j
- Hao, H., Xu, C., Luo, H., Yang, J., Liu, C., Xu, B., et al. (2021). An AIE Luminogen-Based Electropolymerized Film: an Ultrasensitive Fluorescent Probe for TNP and Fe³⁺ in Water. *Mater. Chem. Front.* 5, 492–499. doi:10.1039/d0qm00543f
- Hong, Y., Lam, J. W. Y., and Tang, B. Z. (2011). Aggregation-induced Emission. *Chem. Soc. Rev.* 40, 5361. doi:10.1039/C1CS15113D
- Jiang, Y., Zhang, X., Xiao, L., Yan, R., Xin, J., Yin, C., et al. (2020). Preparation of Dual-Emission Polyurethane/carbon Dots Thermoresponsive Composite Films for Colorimetric Temperature Sensing. *Carbon* 163, 26–33. doi:10.1016/j.carbon.2020.03.013
- Lee, S., Kim, K. Y., Lim, N. Y., Jung, J. H., Lee, J. H., Choi, M. Y., et al. (2019). Terpyridine-based Complex Nanofibers with Eu³⁺ as a Highly Selective Chemical Probes for UO₂²⁺. *J. Hazard. Mater.* 378, 120713. doi:10.1016/j.jhazmat.2019.05.106
- Li, K., Yu, R.-H., Shi, C.-M., Tao, F.-R., Li, T.-D., and Cui, Y.-Z. (2018). Electrospun Nanofibrous Membrane Based on AIE-Active Compound for Detecting Picric

DATA AVAILABILITY STATEMENT

The original contributions presented in the study are included in the article/**Supplementary Material**; further inquiries can be directed to the corresponding author/s.

AUTHOR CONTRIBUTIONS

All authors listed have made a substantial, direct, and intellectual contribution to the work and approved it for publication.

FUNDING

This work was supported by the Guizhou Province Science and Technology Planning Project ((2019)1419, (2019)2845), the Education Department of Guizhou Province (KY(2018)059), the National Natural Science Foundation of China (51803039, 22005224), the Jiangmen City Basic and Theoretical Scientific Research Science and Technology Planning Project (2020JC01019), the Guangdong Basic and Applied Basic Research Funds (2019A1515110944), the Guangdong Science and Technology Major Special Fund (No. 2019-252), the Youth Innovation Talent Project for the Universities of Guangdong Province (2019KQNCX161), and the Wuyi University–Hong Kong/Macau Joint Research Funds (2019WGALH02).

SUPPLEMENTARY MATERIAL

The Supplementary Material for this article can be found online at: <https://www.frontiersin.org/articles/10.3389/fchem.2021.727631/full#supplementary-material>

- Acid in Aqueous Solution. *Sensors Actuators B: Chem.* 262, 637–645. doi:10.1016/j.snb.2018.02.032
- Li, M., Lyu, Q., Sun, L., Peng, B., Zhang, L., and Zhu, J. (2020). Fluorescent Metallosupramolecular Elastomers for Fast and Ultrasensitive Humidity Sensing. *ACS Appl. Mater. Inter.* 12, 39665–39673. doi:10.1021/acsami.0c11278
- Li, W., Ding, Y., Tebyetekerwa, M., Xie, Y., Wang, L., Li, H., et al. (2019). Fluorescent Aggregation-Induced Emission (AIE)-based Thermosetting Electrospun Nanofibers: Fabrication, Properties and Applications. *Mater. Chem. Front.* 3, 2491–2498. doi:10.1039/c9qm00342h
- Liu, Z., Jiang, Z., Yan, M., and Wang, X. (2019). Recent Progress of BODIPY Dyes with Aggregation-Induced Emission. *Front. Chem.* 7, 712. doi:10.3389/fchem.2019.00712
- Luo, J., Xie, Z., Lam, J. W. Y., Cheng, L., Tang, B. Z., Chen, H., et al. (2001). Aggregation-induced Emission of 1-Methyl-1,2,3,4,5-Pentaphenylsilole. *Chem. Commun.* 18, 1740–1741. doi:10.1039/B105159H
- Ma, C., Zhang, X., Yang, L., Li, Y., Liu, H., Yang, Y., et al. (2017). Alkyl Length Dependent Mechanofluorochromism of AIE-Based Phenothiazinyl Fluorophenyl Acrylonitrile Derivatives. *Dyes Pigm.* 136, 85–91. doi:10.1016/j.dyepig.2016.08.031
- Ma, C., Zhang, X., Yang, Y., Ma, Z., Yang, L., Wu, Y., et al. (2016). Effect of Alkyl Length Dependent Crystallinity for the Mechanofluorochromic Feature of Alkyl Phenothiazinyl Tetraphenylethynyl Acrylonitrile Derivatives. *J. Mater. Chem. C* 4, 4786–4791. doi:10.1039/c6tc00939e

- Miao, R., Peng, J., and Fang, Y. (2016). Recent Advances in Fluorescent Film Sensing from the Perspective of Both Molecular Design and Film Engineering. *Mol. Syst. Des. Eng.* 1, 242–257. doi:10.1039/c6me00039h
- Moscoco, F. G., Almeida, J., Sousaraei, A., Lopes-Costa, T., Silva, A. M. G., Cabanillas-Gonzalez, J., et al. (2020). Luminescent MOF Crystals Embedded in PMMA/PDMS Transparent Films as Effective NO₂ gas Sensors. *Mol. Syst. Des. Eng.* 5, 1048. doi:10.1039/c9me00164f
- Peng, X.-X., Bao, G.-M., Zhong, Y.-F., Zhang, L., Zeng, K.-B., He, J.-X., et al. (2021). Highly Sensitive and Rapid Detection of Thiabendazole Residues in Oranges Based on a Luminescent Tb³⁺-Functionalized MOF. *Food Chem.* 343, 128504. doi:10.1016/j.foodchem.2020.128504
- Qin, A., Lam, J. W. Y., and Tang, B. Z. (2012). Luminogenic Polymers with Aggregation-Induced Emission Characteristics. *Prog. Polym. Sci.* 37, 182–209. doi:10.1016/j.progpolymsci.2011.08.002
- Song, N., Chen, D.-X., Xia, M.-C., Qiu, X.-L., Ma, K., Xu, B., et al. (2015). Supramolecular Assembly-Induced Yellow Emission of 9,10-distyrylanthracene Bridged Bis(pillar[5]arene)s. *Chem. Commun.* 51, 5526–5529. doi:10.1039/C4CC08205B
- Sun, X., Wang, Y., and Lei, Y. (2015). Fluorescence Based Explosive Detection: from Mechanisms to Sensory Materials. *Chem. Soc. Rev.* 44, 8019–8061. doi:10.1039/c5cs00496a
- Sun, Z., Yan, F., Xu, J., Zhang, H., and Chen, L. (2021). Solvent-controlled Synthesis Strategy of Multicolor Emission Carbon Dots and its Applications in Sensing and Light-Emitting Devices. *Nano Res.* [Epub ahead of print] doi:10.1007/s12274-021-3495-8
- Thomas, S. W., Joly, G. D., and Swager, T. M. (2007). Chemical Sensors Based on Amplifying Fluorescent Conjugated Polymers. *Chem. Rev.* 107, 1339–1386. doi:10.1021/cr0501339
- Xu, B., Xie, M., He, J., Xu, B., Chi, Z., Tian, W., et al. (2013). An Aggregation-Induced Emission Luminophore with Multi-Stimuli Single- and Two-Photon Fluorescence Switching and Large Two-Photon Absorption Cross Section. *Chem. Commun.* 49, 273–275. doi:10.1039/c2cc36806d
- Xue, J., Wu, T., Dai, Y., and Xia, Y. (2019). Electrospinning and Electrospun Nanofibers: Methods, Materials, and Applications. *Chem. Rev.* 119, 5298–5415. doi:10.1021/acs.chemrev.8b00593
- Yang, H., Sun, Z., Lv, C., Qile, M., Wang, K., Gao, H., et al. (2018). Ratiometric Piezochromism of Electrospun Polymer Films: Intermolecular Interactions for Enhanced Sensitivity and Color Difference. *Chempluschem* 83, 132–139. doi:10.1002/cplu.201800080
- Zhang, X., Zhang, X., Wang, K., Liu, H., Gu, Z., Yang, Y., et al. (2015). A Novel Fluorescent Amphiphilic Glycopolymers Based on a Facile Combination of Isocyanate and Glucosamine. *J. Mater. Chem. C* 3, 1738–1744. doi:10.1039/C4TC02556C
- Zhao, E., Lai, P., Xu, Y., Zhang, G., and Chen, S. (2020a). Fluorescent Materials with Aggregation-Induced Emission Characteristics for Array-Based Sensing Assay. *Front. Chem.* 8, 288. doi:10.3389/fchem.2020.00288
- Zhao, L., Wang, T., Wu, Q., Liu, Y., Chen, Z., and Li, X. (2017a). Fluorescent Strips of Electrospun Fibers for Ratiometric Sensing of Serum Heparin and Urine Trypsin. *ACS Appl. Mater. Inter.* 9, 3400–3410. doi:10.1021/acsami.6b14118
- Zhao, L., Xie, S., Song, X., Wei, J., Zhang, Z., and Li, X. (2017b). Ratiometric Fluorescent Response of Electrospun Fibrous Strips for Real-Time Sensing of Alkaline Phosphatase in Serum. *Biosens. Bioelectron.* 91, 217–224. doi:10.1016/j.bios.2016.12.025
- Zhao, L., Zhang, Z., Liu, Y., Wei, J., Liu, Q., Ran, P., et al. (2020b). Fibrous Strips Decorated with Cleavable Aggregation-Induced Emission Probes for Visual Detection of Hg²⁺. *J. Hazard. Mater.* 385, 121556. doi:10.1016/j.jhazmat.2019.121556
- Zhou, H., Ye, Q., Neo, W. T., Song, J., Yan, H., Zong, Y., et al. (2014). Electrospun Aggregation-Induced Emission Active POSS-Based Porous Copolymer Films for Detection of Explosives. *Chem. Commun.* 50, 13785–13788. doi:10.1039/c4cc06559j
- Zhou, J., Yu, G., and Huang, F. (2017). Supramolecular Chemotherapy Based on Host-Guest Molecular Recognition: a Novel Strategy in the Battle against Cancer with a Bright Future. *Chem. Soc. Rev.* 46, 7021–7053. doi:10.1039/C6CS00898D

Conflict of Interest: The authors declare that the research was conducted in the absence of any commercial or financial relationships that could be construed as a potential conflict of interest.

Publisher's Note: All claims expressed in this article are solely those of the authors and do not necessarily represent those of their affiliated organizations, or those of the publisher, the editors and the reviewers. Any product that may be evaluated in this article, or claim that may be made by its manufacturer, is not guaranteed or endorsed by the publisher.

Copyright © 2021 Ma, Li, Zhang, Xie, Wu, Zhang, Mo, Liu, Wang, Xie and Li. This is an open-access article distributed under the terms of the Creative Commons Attribution License (CC BY). The use, distribution or reproduction in other forums is permitted, provided the original author(s) and the copyright owner(s) are credited and that the original publication in this journal is cited, in accordance with accepted academic practice. No use, distribution or reproduction is permitted which does not comply with these terms.